

## APPENDIX A

Proc. Natl. Acad. Sci. USA  
Vol. 92, pp. 9776-9780, October 1995  
Biochemistry

## Specificity of dimer formation in tropomyosins: Influence of alternatively spliced exons on homodimer and heterodimer assembly

(protein-protein interaction/protein subunit association/united coil/epitope tag)

MARIO GIMONA, AKIYA WATAKABE, AND DAVID M. HELFMAN\*

Cold Spring Harbor Laboratory, 1 Bungtown Road, Cold Spring Harbor, NY 11724

Communicated by Alfred D. Hershey, Cold Spring Harbor Laboratory, Cold Spring Harbor, NY, July 14, 1995

**ABSTRACT** Tropomyosins consist of nearly 100%  $\alpha$ -helix and assemble into parallel and in-register coiled-coil dimers. *In vitro* it has been established that nonmuscle as well as native muscle tropomyosins can form homodimers. However, a mixture of muscle  $\alpha$  and  $\beta$  tropomyosin subunits results in the formation of the thermodynamically more stable  $\alpha/\beta$  heterodimer. Although the assembly preference of the muscle tropomyosin heterodimer can be understood thermodynamically, the presence of multiple tropomyosin isoforms expressed in nonmuscle cells points toward a more complex principle for determining dimer formation. We have investigated the dimerization of rat tropomyosins in living cells by the use of epitope tagging with a 16-aa sequence of the influenza hemagglutinin. Employing transfection and immunoprecipitation techniques, we have analyzed the dimers formed by muscle and nonmuscle tropomyosins in rat fibroblasts. We demonstrate that the information for homo- versus heterodimerization is contained within the tropomyosin molecule itself and that the information for the selectivity is conferred by the alternatively spliced exons. These results have important implications for models of the regulation of cytoskeletal dynamics.

Tropomyosins (TMs) are a family of actin filament-binding proteins that are among the major components of the thin filaments of striated and smooth muscle and the microfilaments of nonmuscle cells (1). Although TMs are expressed in all cells, different isoforms of the protein are characteristic of specific cell types. Isoform diversity of TMs in vertebrate cells is generated by a combination of four genes, multiple promoters, and alternative splicing mechanisms (2-4). We are just beginning to understand the relationship of TM isoform expression and function (5), and although a large number of TM isoforms have been identified, the specific function of these isoforms in different cell types remains to be determined.

The TM subunits consist of nearly 100%  $\alpha$ -helix, and two chains assemble into parallel and in-register coiled-coil dimers (6, 7). TM functions as a dimer and isoform diversity allows a variety of different dimers to be formed. One of the key questions in the understanding of TM function is what mechanisms are responsible for the regulation of the assembly of homo- and heterodimers and whether cell type-specific factors are involved in this process. Rat embryo fibroblasts (REF 52 cell line) express seven nonmuscle TM isoforms simultaneously (refs. 3 and 4; W. Guo and D.M.H., unpublished work): three high molecular weight (HMW) TMs (TM1, TM2, and TM3) and four low molecular weight (LMW) TMs (TM4, TM5, TM5a, and TM5b) of 284 and 248 aa, respectively. Skeletal and smooth muscle  $\alpha$  and  $\beta$  TM subunits preferentially assemble into the thermodynamically more stable  $\alpha/\beta$

heterodimers (8-10). By contrast, studies of TMs from fibroblasts demonstrate that these isoforms exist as homodimers (11, 12), suggesting a more complex principle for determining the formation and stabilization of a specific and functional dimer. Because specificity is determined additionally by the relative thermodynamic stability of all possible protein-protein interactions, understanding this process requires identification of the forces that stabilize preferentially the favored complex as well as forces that destabilize the incorrect one (13). Several groups have addressed the question of homo- versus heterodimer formation, using purified muscle (10, 14, 15) or nonmuscle (11, 12) TMs. However, all of these approaches required either denaturation (10, 14) or chemical stabilization (11, 12, 16) of the TM chains. Thus, these approaches might not identify the possible involvement of cellular factors in the selective formation of TM dimers. This type of assay also seemed not to be suitable for identifying the state and composition of the TM dimers prior to the chemical and thermal treatment. In addition, isoform-specific antibodies are not available for all the isoforms expressed in a single nonmuscle cell, thereby hindering the ability to recover specific TMs in order to identify the subunits present in a given dimer.

In the present study we have used living cells as a system to generate TMs containing the correct set of posttranslational modifications essential for the correct function of TM (17-24). We investigated the dimerization of TMs in cultured cells by epitope tagging with a 16-aa sequence of influenza hemagglutinin (HA-tag) (25, 26) to allow the identification of the native composition of TM homo- and heterodimers. We used immunoprecipitation from extracts of transiently transfected REF 52 cells at low temperature, where chain exchange is minimized (14), to analyze the composition of the dimers. We demonstrate that the information for homo- versus heterodimerization is contained within the TM molecule itself and that the information for the selectivity is conferred by the alternatively spliced exons.

### EXPERIMENTAL PROCEDURES

**Construction of Transfection Plasmids.** All TM constructs were cloned in-frame between *Xba* I and *Bam*HI sites in the pCGN expression vector (27) with or without the 16-aa HA-tag sequence. Primers were 5'-ATGGACGCCATCAAGAGAAG-3' for TM1, TM2, TM3, smooth muscle  $\alpha$ -TM, and skeletal muscle  $\alpha$ -TM; 5'-ATGGCCGGCCTCAACTCATCG-3' for TM4; and 5'-ATGGCCGGGTAGCTCGCTG-3' for TM5a and TM5b. Each tagged TM therefore carried the HA-tag sequence at its amino terminus.

Abbreviations: TM, tropomyosin; HMW, high molecular weight; LMW, low molecular weight; HA, hemagglutinin.

\*To whom reprint requests should be addressed at: Cold Spring Harbor Laboratory, P.O. Box 100, Cold Spring Harbor, NY 11724.

The publication costs of this article were defrayed in part by page charge payment. This article must therefore be hereby marked "advertisement" in accordance with 18 U.S.C. §1734 solely to indicate this fact.

**Immunofluorescence.** Rat embryo fibroblast (REF 52) cells grown to 75% confluence in Dulbecco's modified Eagle's medium with 10% fetal bovine serum were transfected with 1  $\mu$ g of total DNA per construct and 25  $\mu$ l of Lipofectamine (GIBCO) per 60-mm dish for 24 hr and prepared for immunofluorescence as described (28). Tagged TMs were visualized with anti-HA antibody 12CA5 and rhodamine-conjugated goat anti-mouse secondary antibody (Molecular Probes). Fluorescent images were photographed on a Zeiss Axiophot microscope using a  $\times 63$  oil-immersion lens and Kodak P3200 Tmax film. The transfection efficiency in REF 52 cells was observed to be at around 10% with the Lipofectamine method.

**Immunoprecipitation.** REF 52 cells after 24 hr of transfection were washed three times with ice-cold phosphate-buffered saline (pH 7.4) containing 5 mM  $MgCl_2$  and 2 mM EGTA. Proteins for immunoprecipitation were extracted in 200  $\mu$ l of IP buffer (20 mM imidazole/300 mM KCl/5 mM  $MgCl_2$ /5% (vol/vol) glycerol/1% (vol/vol) Triton X-100/1 mM phenylmethanesulfonyl fluoride/1 mM  $NaN_3$ /1 mM ATP, pH 7.0) per 60-mm dish for 60 min on ice. Cellular residue was removed by centrifugation and the extract was precleared for 60 min with protein A-Sepharose (Pharmacia) in IP buffer. The supernatant was transferred to a fresh tube washed twice for 5 min in IP buffer to reduce nonspecific binding. Five micrograms of 12CA5 antibody was added and the suspension was incubated on ice for 60 min. After addition of 30  $\mu$ l of protein A-Sepharose, incubation was continued for another 60 min. The beads were washed three times in IP buffer and once in phosphate-buffered saline and then prepared for gel electrophoresis.

**Electrophoresis and Western Blotting.** Analytical SDS/12.5% PAGE in mini-slab gels and Western blotting onto nitrocellulose (Hybond, Amersham) were performed as described (29). Transferred proteins were visualized with a horseradish peroxidase-coupled secondary antibody and the ECL chemiluminescence detection system (Amersham).

**Antibodies.** Monoclonal anti-TM antibody (clone 311) that recognizes all the HMW TMs was from Sigma. Monoclonal anti-HA antibody (clone 12CA5; refs. 25 and 26) was produced as mouse ascites fluid in Cold Spring Harbor. Monoclonal anti-TM antibody (clone MP10) that recognizes the low molecular weight TMs was kindly provided by Mark Pittenger (Cold Spring Harbor Laboratory).

## RESULTS

**Cell Transfection.** We have used the expression vector pCGN (Fig. 1A) for the transfection of mammalian cells with each of the nine rat TM isoforms, which are the products of the three genes depicted in Fig. 1B. Each TM was expressed either with or without an amino-terminal 16-aa HA-tag. Transfected rat embryo fibroblast (REF 52) cells expressed significant amounts of the tagged TM isoforms, and no premature chain-termination products were detected by Western blotting (Fig. 2). The ratio of exogenous TM subunits to the major endogenous TM subunit (TM1 in REF 52 cells) was determined to be at about 1:1. This value represents a semiquantitative estimate from Western blots of total cell extracts (with an estimated transfection efficiency of 10%) and is therefore not equivalent to the situation found in every single cell. Further, the levels of expression (as determined by immunofluorescence) additionally varied by a factor of  $\sim 20$ , and cells expressing very high amounts of tagged TM contained large cisternal structures filled with immunoreactive material (data not shown).

**Incorporation of Tagged TM Isoforms into Actin Stress Fibers.** Tagged TMs were incorporated into the actin-containing stress fibers of REF 52 cells within 24 hr after transfection. The immunofluorescent patterns obtained with the 12CA5 antibody (Fig. 3) are comparable with those seen

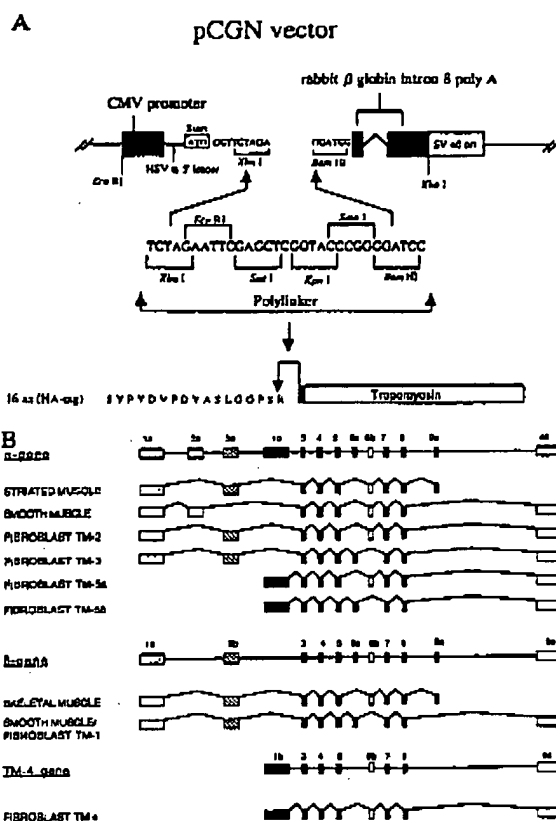


FIG. 1. (A) Mammalian expression vector pCGN. From left to right, labeled features include the human cytomegalovirus (CMV) promoter, the herpes simplex virus (HSV) thymidine kinase (tk) gene 5' untranslated leader and initiation codon, the unique *Xba* I site engineered downstream of the initiation codon, the engineered *Bam*HI site, the rabbit  $\beta$ -globin gene segment containing splicing and poly(A)-addition signals, and the simian virus 40 (SV 40) origin of replication (ori). (B) Intron-exon organization of the rat TM genes and spliced TM isoforms used for transfection. Nonmuscle cells express multiple isoforms of 284 aa (TM1, TM2, and TM3) and 248 aa (TM4, TM5a, and TM5b) simultaneously, whereas muscle cells express either one (the  $\alpha$  isoform in cardiac muscle) or two (both  $\alpha$  and  $\beta$  chains in smooth or skeletal muscle) of the HMW type.

with TM-specific antibodies (30). Thus, the tag sequence at the amino terminus did not interfere with the ability of the TMs to associate with F-actin bundles. The HA-tagged TMs were also expressed in and purified from *Escherichia coli* and were found to cosediment with F-actin in an *in vitro* cosedimentation assay with rabbit skeletal muscle F-actin (data not shown). This result is consistent with previous studies demonstrating that wild-type recombinant TM was incorporated into stress fibers whether it was unacetylated (30, 31) or blocked by an 80-residue amino-terminal fusion (31) and that the patterns of

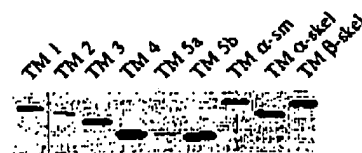


FIG. 2. Western blotting of whole cell extracts with anti-HA antibody 12CA5 demonstrating the high amounts of tagged TM isoforms present in transfected REF 52 cells.

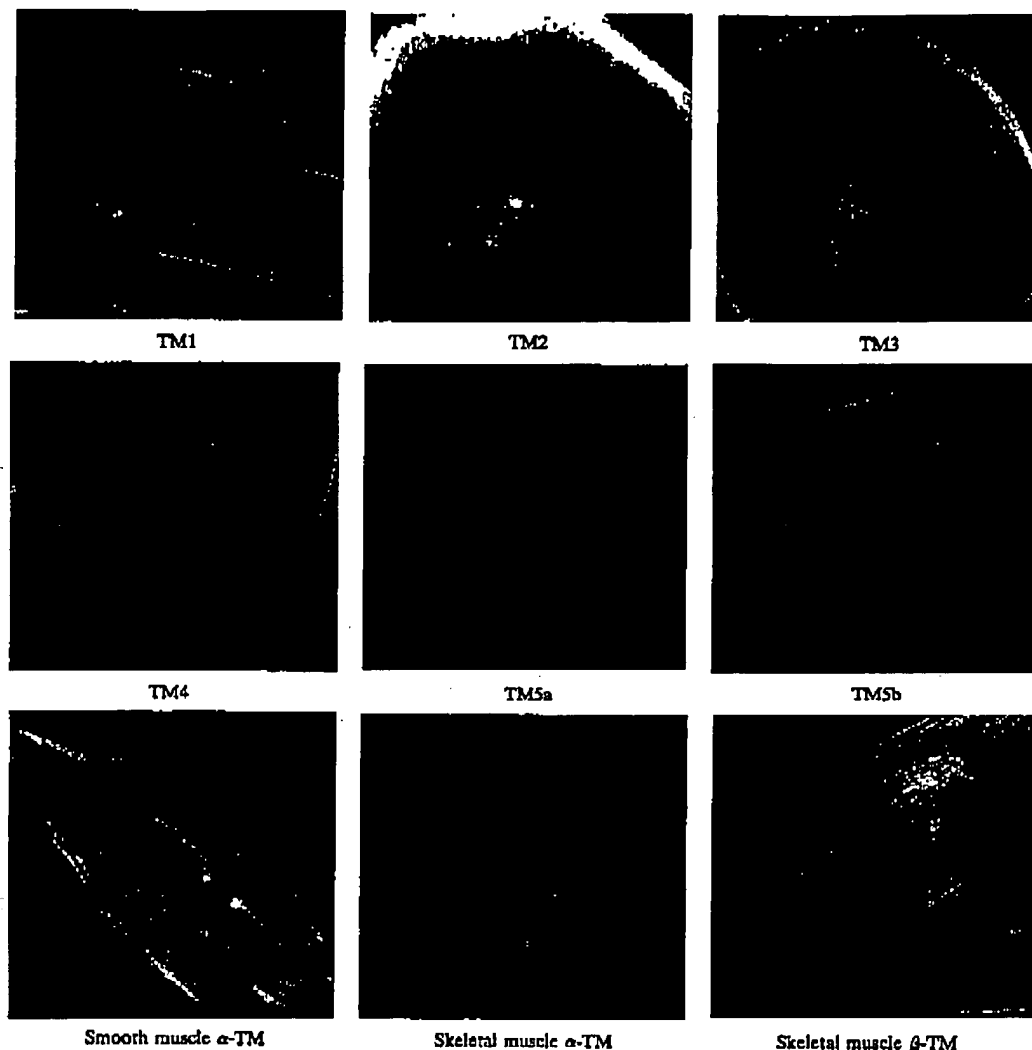


FIG. 3. Immunofluorescence showing that all HA-tagged isoforms localize and integrate into the actin-containing stress fibers of REF 52 cells. (Bar = 20  $\mu$ m.)

incorporated TM were indistinguishable from that of endogenous TM (30) or isolated chicken pectoral muscle TM (31).

**Dimer Formation.** The transient expression of HA-tagged or untagged exogenous TM isoforms in REF 52 cells allows the formation of a variety of dimers in addition to the dimers present in the untransfected cells (Fig. 4A). Besides the native homo- or heterodimers containing the endogenous TM chains (I), hybrid dimers containing either one (II) or two (III) tagged exogenous TM chains are possible. In addition, in double transfections where one tagged isoform and one untagged isoform are introduced into cells simultaneously, the formation of "native hybrids" containing two untagged chains, one endogenous and one exogenous, are possible. The differences in electrophoretic mobility due to the presence of the 16-aa tag allow the identification of both homodimers and heterodimers by SDS/12.5% PAGE. When extracts from metabolically  $^{35}$ S-labeled transfected REF 52 cells were separated in SDS/12.5% polyacrylamide gels and autoradiographed, the expression of the tagged TM chains in these cells 24 hr after

transfection was seen to be comparable to that of the endogenous TMs. Immunoprecipitations from these cell extracts further revealed that the tagged TMs were precipitated in equal amounts by the anti-HA antibody and that actin contamination was negligible (data not shown).

Western blot analysis of the immunoprecipitated tag-containing dimers demonstrated the preference of the 284-aa HMW nonmuscle isoforms TM1, TM2, and TM3 to form homodimers (Fig. 4B). REF 52 cells express the three HMW TM isoforms in different amounts (TM1 > TM2 >> TM3). To eliminate problems due to differential amounts of exogenous and endogenous TMs present in the extracts, cotransfections were performed with the same expression vector introducing the same TM subunit both tagged and untagged into the cells. Cotransfections of tagged TM constructs in parallel with untagged TMs did not alter the homodimer preference of the HMW nonmuscle isoforms (Fig. 4C).

Since fibroblast TM2 differs from smooth muscle  $\alpha$ -TM or skeletal muscle  $\alpha$ -TM by the use of exons 2a/2b or 9a/9d,

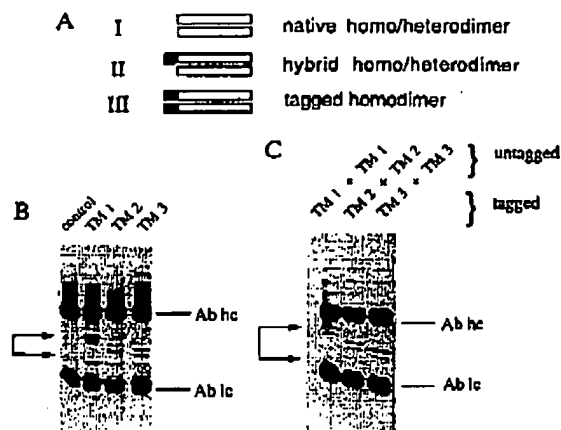


FIG. 4. (A) Contribution of the different possible dimers to the bands analyzed in SDS/polyacrylamide gels (see text). Open bars symbolize the TM chains; black boxes indicate the presence or absence of the HA-tag sequence. (B) Western blot analysis of anti-HA (12CA5) immunoprecipitates probed with a monoclonal antibody recognizing all HMW TMs (clone 311; Sigma). Single transfections of REF 52 cells with each of the nonmuscle HMW TM variants resulted in the precipitation of predominantly homodimers of the respective TM subunits. The presence of the 16-aa HA-tag increases the apparent molecular mass of the monomer chain by ~2 kDa, allowing the identification of both tagged (upper band) and untagged (lower band) TMs according to their mobility in SDS/12.5% polyacrylamide gels. Two strongly reacting bands represent the reaction of the heavy (Ab hc) and light (Ab lc) chains of the added 12CA5 antibody with the goat anti-mouse secondary antibody. Area between arrows indicates position of TMs. When an extract of untransfected cells was used (control), no TMs were identified in the immunoprecipitate. (C) Double transfections using both one tagged and one untagged HMW isoform resulted in the precipitation of homodimers.

respectively (see Fig. 1B), it was possible that these alternatively spliced exons were critical for the selective formation of homo- versus heterodimers. When tagged smooth muscle  $\alpha$ -TM or skeletal muscle  $\alpha$ -TM isoforms were cotransfected with untagged HMW nonmuscle TM isoforms, the formation of heterodimer was predominant (Fig. 5A and B). Similarly, skeletal muscle  $\beta$ -TM formed heterodimers with TM1, TM2,

and TM3 (Fig. 5A and B). Thus, the muscle isoforms were capable of shifting the dimer equilibrium in the direction of the heterodimer. The selectivity of the dimer formation was further indicated by the results obtained with combinations of HMW and LMW TM isoforms. Tagged smooth muscle  $\alpha$ -TM, skeletal muscle  $\beta$ -TM, or nonmuscle TM2 failed to form stable heterodimers with cotransfected LMW nonmuscle variant TM4, TM5a, or TM5b (Fig. 5C).

## DISCUSSION

Coiled coils are found as stabilizing motifs in many different types of dimeric proteins. In the case of the basic region-leucine zipper (bZIP) family of transcription factors, Lumb and Kim (32) demonstrated that the dimerization into parallel coiled-coil dimers was controlled by the leucine zipper sequence. Similarly, O'Shea *et al.* (13) identified 8 residues in the 35-aa leucine zipper region of the oncoproteins Fos and Jun as the essential determinants for their heterodimerization into parallel, two-stranded coiled coils and demonstrated that the driving force for preferential heterodimer formation was the destabilization of the Fos homodimer. In addition, neurotrophins have been shown to be biologically active as noncovalently linked homodimers. Recently, Heymach and Shooter (33) have used a technique similar to the one applied in this work to show that three members of the neurotrophin family (nerve growth factor, brain-derived neurotrophic factor, and neurotrophin 3) were able to form heterodimers upon forced expression following transfection of cells. Our results demonstrate that amino- and carboxyl-terminal regions, as well as internal regions, contribute to the coiled-coil interactions of the TM subunits.

There is general agreement that the  $\alpha$ -helical TM molecule unfolds and dissociates in parallel during a heating experiment, indicating regions of varying stability or many states of partially unfolded molecules. The unfolding of heterodimers is expected to be even more complex than that of homodimers, since not only domains or states of heterodimers are involved, but homodimer domains (or states) also contribute to the equilibrium state (34). In a CD study of *Rana esculenta*  $\alpha/\beta$  TM, two major helix-coil transitions were observed which have been interpreted as the unfolding of independent domains (34). Ishii *et al.* (35, 36) have demonstrated that recombinant TMs carrying an amino-terminal fusion peptide are still

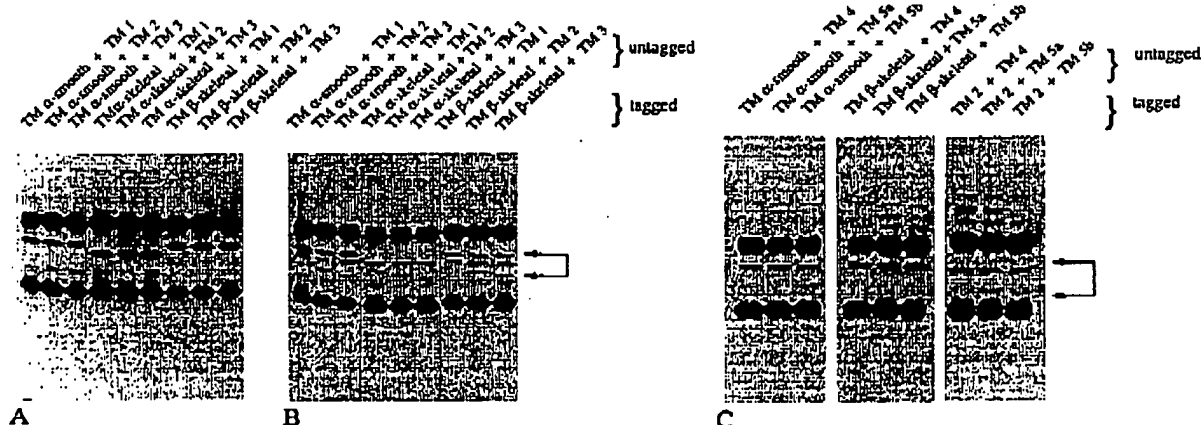


FIG. 5. (A and B) Cotransfections using HA-tagged muscle isoforms in combination with untagged HMW nonmuscle isoforms resulted in the predominant formation of stable heterodimers. Western blots of anti-HA immunoprecipitates were probed with anti-HA antibody 12CA5 (A) and anti-TM antibody 311 (B). (C) When either muscle TMs or a HMW nonmuscle TM (TM2) was cotransfected with LMW nonmuscle TMs, however, no stable dimers were precipitated. Western blot probed with a mixture of antibodies 12CA5 and MP10 (gift of Mark Pittenger; recognizes low molecular weight TMs). Area between arrows indicates position of TMs.

close together for local unfolding while they are separated for global unfolding. The conformation of the local unfolded region and the mechanism of the local unfolding of TM remained unsolved, however.

Whereas rat muscle cells express only one (cardiac) or two (smooth and skeletal) isoforms of TM, up to seven different TMs are present in a single rat fibroblast (refs. 4 and 30; W. Guo and D.M.H., unpublished work). We have shown that the presence of the amino-terminally tagged transfected muscle isoforms in a nonmuscle cell leads to the formation of heterodimers between endogenous and exogenous HMW non-muscle TMs. Muscle-specific factors cannot be involved in the process of the formation (or stabilization) of heterodimers since this process is taking place in a cultured nonmuscle cell. Nonmuscle-specific factors were also not effective in maintaining the homodimeric state of the endogenous nonmuscle TMs in the presence of the transfected muscle isoforms.

Different TM isoforms differ in binding to troponin T, the formation of head-to-tail overlaps, and their affinity for F-actin (reviewed in refs. 3 and 4). A relationship between alternatively spliced exons and functional domains in TMs was found by investigating the influence of exons 2a/b and 9a/d of the smooth and striated  $\alpha$ -TMs (5). Although the presence of exon 9a was correlated with  $\text{Ca}^{2+}$ -insensitive binding to troponin and the presence of exon 2a was correlated with changes in actin affinity, the individual exons were not recognizable as individual structural domains (5). Expression of chimeric TMs in fibroblasts recently indicated that a coordination between the amino- and carboxyl-terminal regions is required for normal TM function (37). Our data support this latter assumption and suggest that coordination between several domains in TMs is responsible for the formation of functionally relevant TM dimers. Exons 3-5, 7, and 8 are common to all TMs and appear from our studies to be insufficient to warrant stable dimerization *per se*, since stable heterodimers between LMW and HMW TMs were not observed under our assay conditions. Whether or not changes in the sequences of these conserved domains could lead to perturbation of the dimeric interactions of TM subunits is unknown. Additionally, it will be interesting to determine the influence of exon 1b (used in the 248-aa subunits of TM4, TM5, TM5a, and TM5b) on the dimerization properties of the LMW isoforms.

The functional significance of expressing a multitude of TM isoforms in nonmuscle cells and maintaining them as homodimers remains to be determined. The higher actin-binding ability of strongly head-to-tail overlapping heterodimers of smooth muscle  $\alpha$  and  $\beta$  TM subunits in chicken gizzard might reflect the necessity to maintain stable association with the muscle thin filament throughout the entire length of the actin filament. For chicken gizzard TM, the heterodimer exhibits a greater ability to bind cooperatively to F-actin, due to its stronger head-to-tail overlap as compared with the  $\alpha/\alpha$  and  $\beta/\beta$  homodimers. It has also been suggested that the TM heterodimers represent a more flexible structure than their homodimeric counterparts (38). A higher end-to-end association of TM heterodimers in smooth muscle cells could lead to the formation of elongated TM polymers, which could reflect the requirement for a higher degree of flexibility to accommodate the structural changes in the F-actin filament during contraction and relaxation cycles (38). In contrast, a reduced ability of the homodimers to associate head-to-tail could be a necessary determinant for the more dynamic regulation of the actin cytoskeleton in nonmuscle cells.

We are grateful to Dr. Kathleen Collins for critical and valuable comments on the manuscript and Dr. Mark Pittenger for the MP10 antibody. The photographic assistance of Phil Renna, Jim Duffy, and

Michael Ockler is gratefully acknowledged. M.G. is an Erwin Schrödinger fellow of the Austrian Fonds zur Förderung der Wissenschaftlichen Forschung (Project J-09020 MOB). A.W. received a Human Frontier fellowship. D.M.H. is supported by National Cancer Institute Grant CA58607 and is an Established Investigator of the American Heart Association.

1. Leavis, P. C. & Gergely, J. (1984) *CRC Crit. Rev. Biochem.* 16, 235-305.
2. Goodwin, L. O., Lees-Miller, J. P., Cheley, S., Leonard, M., & Helfman, D. M. (1991) *J. Biol. Chem.* 266, 8408-8415.
3. Lees-Miller, J. P. & Helfman, D. M. (1991) *BioEssays* 13, 429-437.
4. Pittenger, M. F., Kazzaz, J. A., & Helfman, D. M. (1994) *Curr. Opin. Cell Biol.* 6, 96-104.
5. Cho, Y.-J. & Hitchcock-DeGregori, S. E. (1991) *Proc. Natl. Acad. Sci. USA* 88, 10153-10157.
6. Gracetta, P. (1989) *Biochemistry* 28, 1282-1287.
7. Whitby, F. G., Kent, H., Stewart, F., Stewart, M., Xie, X., Hatch, V., Cohen, C., & Phillips, G. N., Jr. (1992) *J. Mol. Biol.* 227, 441-452.
8. Brown, H. R. & Schachar, F. H. (1985) *Proc. Natl. Acad. Sci. USA* 82, 2359-2363.
9. Lehrer, S. S. & Qian, Y. (1990) *J. Biol. Chem.* 265, 1134-1138.
10. Jancsó, A. & Gracetta, P. (1991) *J. Biol. Chem.* 266, 5891-5897.
11. Lin, J. J.-C., Helfman, D. M., Hughes, S. H., & Chou, C. S. (1985) *J. Cell Biol.* 100, 692-703.
12. Matsumura, F. & Yamashiro-Matsumura, S. (1985) *J. Biol. Chem.* 260, 13851-13859.
13. O'Shea, O. K., Rutkowski, R., & Kim, P. S. (1992) *Cell* 68, 699-708.
14. Lehrer, S. S., Qian, Y., & Hvidt, S. (1989) *Science* 246, 926-928.
15. Sanders, C., Burnick, L. D., & Smilie, L. B. (1986) *J. Biol. Chem.* 261, 12774-12778.
16. Gracetta, P. (1992) *Biochim. Biophys. Acta* 1120, 205-207.
17. Pan, B.-S., Gordon, A. M., & Potter, J. D. (1991) *J. Biol. Chem.* 266, 12432-12438.
18. Monteiro, P. B., Lararo, R. C., Ferro, J. A., & Reinach, F. C. (1994) *J. Biol. Chem.* 269, 10461-10466.
19. Greenfield, N. J., Stafford, W. F., & Hitchcock-DeGregori, S. E. (1994) *Protein Sci.* 3, 402-410.
20. Heald, R. W., & Hitchcock-DeGregori, S. E. (1988) *J. Biol. Chem.* 263, 5254-5259.
21. Urbancikova, M., & Hitchcock-DeGregori, S. E. (1994) *J. Biol. Chem.* 269, 24310-24315.
22. Heeley, D. H. (1994) *Eur. J. Biochem.* 221, 129-137.
23. Heeley, D. H., Watson, M. A., Mak, A. S., Dubord, P., & Smilie, L. B. (1989) *J. Biol. Chem.* 264, 2424-2430.
24. Cho, Y.-J., Liu, J., & Hitchcock-DeGregori, S. E. (1990) *J. Biol. Chem.* 265, 538-545.
25. Kolodziej, P. A., & Young, R. A. (1991) *Methods Enzymol.* 194, 508-519.
26. Niman, H. L., Houghten, R. A., Walker, L. E., Reisfeld, R. A., Wilson, I. A., Hogle, J. M., & Lerner, R. A. (1983) *Proc. Natl. Acad. Sci. USA* 80, 4949-4953.
27. Tanaka, M., Lai, J. S., & Herr, W. (1992) *Cell* 68, 755-767.
28. Small, J. V. (1988) *Electron Microsc. Rev.* 1, 155-174.
29. Gimona, M., Herzog, M., Vandeckerckhove, J., & Small, J. V. (1990) *FEBS Lett.* 274, 159-162.
30. Pittenger, M. F., & Helfman, D. M. (1992) *J. Cell Biol.* 118, 841-858.
31. Ranucci, D., Yamakita, Y., Matsumura, F., & Hitchcock-DeGregori, S. E. (1993) *Cell Motil. Cytoskeleton* 24, 119-128.
32. Lumb, K. J., & Kim, P. S. (1995) *Science* 268, 436-439.
33. Heymach, J. V., Jr., & Shooter, E. M. (1995) *J. Biol. Chem.* 270, 12297-12304.
34. Hvidt, S., & Lehrer, S. S. (1992) *Biophys. Chem.* 45, 51-59.
35. Ishii, Y., Lehrer, S. S., & Hitchcock-DeGregori, S. E. (1990) *Biophys. J.* 57, 154a (abstr.).
36. Ishii, Y. (1994) *Eur. J. Biochem.* 221, 705-712.
37. Warren, K. S., Lin, J. J.-C., McDermott, J. P., & Lin, J. J.-C. (1995) *J. Cell Biol.* 129, 697-708.
38. Cheung, R., & Censullo, H. C. (1994) *J. Mol. Biol.* 243, 520-529.

## Kinetics Control Preferential Heterodimer Formation of Platelet-derived Growth Factor from Unfolded A- and B-chains\*

Received for publication, December 4, 2002, and in revised form, February 26, 2003  
Published, JBC Papers in Press, March 3, 2003, DOI 10.1074/jbc.M212317200

Carsten Müller‡, Susanne Richter§, and Ursula Rinas¶

From the GBF National Research Center for Biotechnology, Biochemical Engineering Division, Mascheroder Weg 1, 38124 Braunschweig, Germany

The folding and assembly of platelet-derived growth factor (PDGF), a potent mitogen involved in wound-healing processes and member of the cystine knot growth factor family, was studied. The kinetics of the formation of disulfide-bonded dimers were investigated under redox reshuffling conditions starting either from unfolded and reduced PDGF-A- or B-chains or an equimolar mixture of both chains. It is shown that in all cases the formation of disulfide-bonded dimers is a very slow process occurring in the time scale of hours with a first-order rate-determining step. The formation of disulfide-bonded PDGF-AA or PDGF-BB homodimers displayed identical kinetics, indicating that both monomeric forms as well as the dimerized homodimer have similar folding and assembly pathways. In contrast, the formation of the heterodimer occurred three times more rapidly compared with the formation of the homodimers. As both monomeric forms revealed similar renaturation kinetics, it can be concluded that the first-order rate-determining folding step does not occur during monomer folding but must be attributed to conformational rearrangements of the dimerized, not yet disulfide-bonded protein. These structural rearrangements allow a more rapid formation of intermolecular disulfide bonds between the two different monomers of a heterodimer compared with the formation of the disulfide bonds between two identical monomers. The preferential formation of disulfide-bonded heterodimers from an equimolar mixture of unfolded A- and B-chains is thus a kinetically controlled process. Moreover, similar activation enthalpies for the formation of all different isoforms suggest that faster heterodimerization is controlled by entropic factors.

a non-glycosylated protein that belongs to the family of dimeric cystine knot growth factors (5). The PDGF family consists of different gene products. The most prominent and long known members of this family are PDGF-A and -B. More recently, two new less abundant members, PDGF-C and -D, have been discovered (6, 7).

The two different homologous monomers of PDGF, denoted as A- and B-chains, are known to exist in the three natural occurring dimeric isoforms PDGF-AA, -AB, and -BB (8, 9). These different isoforms have apparently distinct biological functions indicated, e.g. by their different binding affinities to the two different types of PDGF receptors (10). However, the majority of PDGF purified from human platelets is the disulfide-bonded heterodimeric growth factor (11), suggesting that heterodimerization is favored when both genes are coexpressed. Also, PDGF-AB disulfide-bonded heterodimers are almost exclusively formed from an equimolar mixture of unfolded and reduced A- and B-chains when renaturation is carried out under conditions that allow disulfide bond reshuffling (12–14).

From all potential isoforms of the PDGF dimer, only the structure of the BB homodimer has been determined so far (Fig. 1; Ref. 15). PDGF-BB is an all- $\beta$  sheet protein of about 30 kDa and composed of two very flat subunits arranged head-to-tail and linked together by two intermolecular disulfide bonds (5, 15). In addition to intermolecular disulfide bonds, each monomer contains an unusual knot-like arrangement of three intramolecular disulfide bridges where one disulfide bond threads through a loop formed by the two other disulfide bonds (5, 15). As all members of the cystine knot growth factor family share strong structural homology, it is most likely that the other PDGF isoforms are of almost identical structure as the BB isoform.

The folding pathways of oligomeric proteins frequently exhibit very complex profiles, since unimolecular folding reactions and bimolecular association steps are involved (16, 17). In case of PDGF, the folding and association process becomes even more complex through the additional requirement for the formation of the unusual knot-like arrangement of the three intramolecular disulfide bridges and the formation of the two intermolecular disulfide bonds. Although many members of the cystine knot growth factor family are of enormous medical importance (e.g. PDGFs, transforming growth factors, bone morphogenetic proteins), almost no knowledge exists about the mechanisms governing their folding and assembly. Some more detailed studies have been carried out on the folding and association kinetics of brain-derived neurotrophic factor (18) and nerve growth factor (19). Both factors belong to a subgroup of the cystine knot growth factor family where the subunits are not connected by intermolecular disulfide bonds in the dimeric protein. Kinetic studies on the folding and assembly of those growth factors of the cystine knot family where the subunits are connected by disulfide

Platelet-derived growth factor (PDGF)<sup>1</sup> is a potent mitogen for cells of mesenchymal origin, i.e. smooth muscle cells, connective tissue cells, or blood cells (1–3). It is released by platelets upon wounding and plays an important role in stimulating adjacent cells to grow and thereby heal the wound (4). PDGF is

\* The costs of publication of this article were defrayed in part by the payment of page charges. This article must therefore be hereby marked "advertisement" in accordance with 18 U.S.C. Section 1734 solely to indicate this fact.

‡ Current address: Aventis Pharma Deutschland GmbH, 65926 Frankfurt, Germany.

§ Current address: CytoS Biotechnology AG, Wagistrasse 25, 8952 Zurich-Schlieren, Switzerland.

¶ To whom correspondence should be addressed. Tel.: 49-531-6181-126; Fax: 49-531-6181-111; E-mail: URI@gbf.de.

<sup>1</sup> The abbreviations used are: PDGF, platelet-derived growth factor; CdnHCl, guanidinium hydrochloride; SEC, size exclusion chromatography.

## Preferential Heterodimer Formation of Platelet-derived Growth Factor

18331

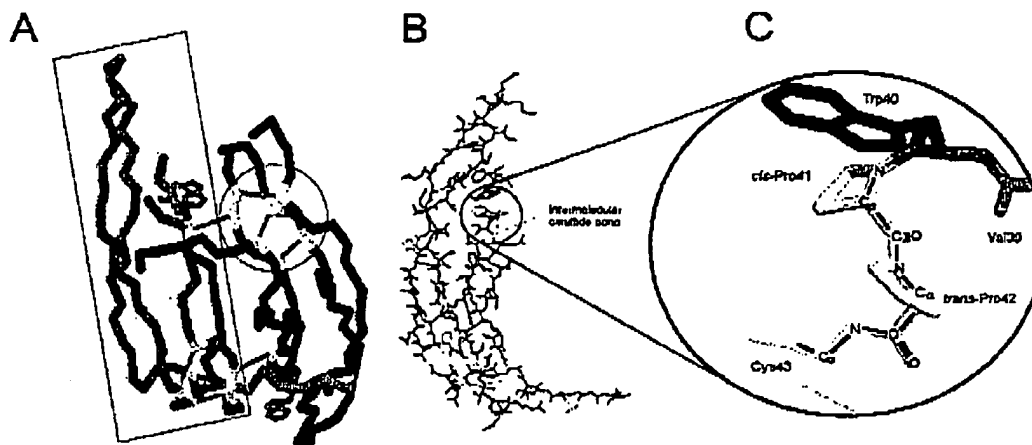


FIG. 1. Schematic presentation of the three-dimensional structure of PDGF-BB. A, the two monomers (depicted in green and blue) are connected head-to-tail via two intermolecular disulfide bonds. Each monomer contains a knot-like arrangement of three intramolecular disulfide bonds, where two disulfide bonds connect two  $\beta$ -strands and form a ring structure, and the third disulfide bond threads through this ring and connects two additional  $\beta$ -strands. The positions of the cysteines are indicated in yellow. The disulfide bonds are shown in red. The single tryptophan is indicated in violet. The gray rectangle underlays the area occupied by one subunit and the gray circle the position of the cysteine knot in the other subunit. B, bowl-like structure of a single subunit with the positions of the prolines indicated in gray. C, close-up of the local backbone conformation in the vicinity of the conserved cysteine (Cys<sup>43</sup>) involved in intermolecular disulfide-bonding. All solved structures of members of the cystine knot growth factor family show evidence for the presence of a conserved *cis*-proline (Ref. 15: PDGF-BB, Trp<sup>40</sup>-Pro<sup>41</sup>-*cis*-Pro<sup>41</sup>-Cys<sup>43</sup>; Refs. 30 and 31). The same motif is also present in the PDGF-A chain (PDGF-A, Trp<sup>40</sup>-Pro<sup>41</sup>-Pro<sup>42</sup>-Cys<sup>43</sup>), although the structures of PDGF-AA or PDGF-AB have not yet been determined.

bonds in the native protein are missing so far.

It was commonly accepted that the presence of the cystine knot is a prerequisite for the dimerization of proteins belonging to the cystine knot growth factor family (5). However, recent studies on the structure and stability of vascular endothelial growth factor, a member of PDGF superfamily of cystine knot growth factors, revealed that cystine deletion mutants lacking one of the two disulfide bonds forming the outer ring of the knot motif are still able to form disulfide-bonded dimers (20). Surprisingly, these mutants even revealed an increased thermodynamic stability although their thermal stability was severely reduced (20). However, the formation of the cystine knot appears to be indispensable for the biological activity of PDGF (21), while the intermolecular disulfide bridges have a stabilizing but non-essential effect on the biological activity (21, 22). PDGF is very prone to aggregation when renaturation is initiated by diluting unfolded and reduced monomers into a buffer, which allows refolding and disulfide bond reshuffling (14). Once folded, however, PDGF is a very stable protein withstanding temperatures of up to 100 °C (23).

Previously, we have presented a renaturation method based on the utilization of size exclusion chromatography, which circumvents aggregation during refolding and allows renaturation of PDGF at high protein concentrations (14). In this study, we present a kinetic analysis of the formation of disulfide-bonded dimers and propose a model for the folding pathway of the different isoforms of PDGF. The unfolded and reduced monomers of PDGF were subjected to size exclusion chromatography under renaturing conditions and the formation of disulfide-bonded dimers starting either from pure A- or B-chains or an equimolar mixture of both monomeric isoforms was followed in the eluate fraction.

## EXPERIMENTAL PROCEDURES

**PDGF-BB Structure Visualization.** PDGF-BB structure data were obtained from the Protein Data Bank ([www.rcsb.org/pdb/](http://www.rcsb.org/pdb/); accession number 1pdg) and visualized using the program RasMol, Version 2.7.2.1 (RasMol Molecular Renderer; R. Sayle, Glaxo Research and Development Greenford, Middlesex, UK).

**Production and Purification of PDGF Isoforms.** The different PDGF isoforms were produced as inclusion bodies using the *Escherichia coli* strain TG1 carrying temperature-inducible expression vectors encoding either the PDGF A- or B-chain or a bicistronic vector encoding both chains synthesized in a 1:1 ratio upon induction (13). Production of PDGF was carried out in a high cell density cultivation procedure that has been described previously (24). Purification of unfolded and reduced PDGF monomers from solubilized PDGF containing inclusion bodies was done by size exclusion chromatography (SEC) under denaturing conditions (14).

**Kinetic Analysis of PDGF Dimerization.** Purified, unfolded, and reduced PDGF monomers (either pure A-, or B-chains, or an equimolar mixture of the two chains) were subjected to SEC under conditions that allow refolding and reshuffling of disulfide bridges as described previously (14). Standard renaturation conditions by SEC were: 1 mol l<sup>-1</sup> Tris-HCl (pH 7.8), 0.5 mol l<sup>-1</sup> guanidinium hydrochloride (GdnHCl), 10 mmol l<sup>-1</sup> glutathione reduced (GSH), 0.25 mmol l<sup>-1</sup> glutathione oxidized (GSSG). Under these conditions, the eluted PDGF monomers were able to dimerize in the eluate fraction to yield the dimeric, disulfide-bonded, and biologically active growth factor (14). Aggregation of PDGF during the renaturation procedure was not observed unless otherwise indicated. The formation of disulfide-bonded dimers was followed in aliquots taken from the reaction mixture in the eluate fraction through disulfide trapping by irreversible blocking of free thiol groups and subsequent separation of monomeric and dimeric PDGF by gel electrophoresis under non-reducing conditions. Blocking of the free thiol groups by the addition of iodoacetate and gel electrophoresis was carried out as described previously (14). Gels were stained with Coomassie Brilliant Blue, and quantification of the monomeric and dimeric fraction of PDGF was carried out by densitometry (Hirschman elscript 400).

The putative reaction order for the rate-limiting step during dimerization of PDGF was determined from the slopes of the linearized kinetic equations assuming either a first-order (Equation 1),

$$\ln[A]_t = \ln[A]_0 - \sum \nu_i k_1 t \quad (\text{Eq. 1})$$

or a second-order rate-determining reaction (Equation 2),

$$\frac{1}{[A]_t} - \frac{1}{[A]_0} = \sum \nu_i k_2 t \quad (\text{Eq. 2})$$

where  $[A]_t$  and  $[A]_0$  are the monomer concentrations at times  $t$  and zero, respectively,  $\sum \nu_i$  is the sum of the stoichiometric factors, and  $k_1$  and  $k_2$  are the rate constants for a first- or second-order reaction, respectively.

18332

## Preferential Heterodimer Formation of Platelet-derived Growth Factor

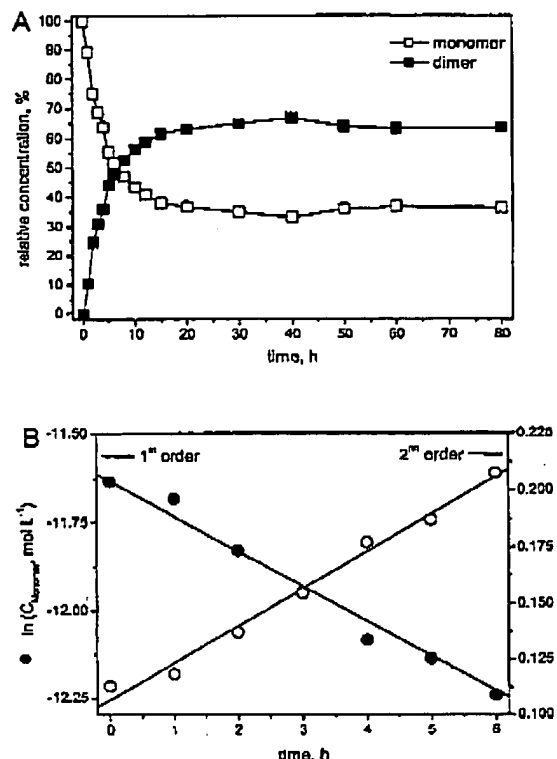


FIG. 2. Kinetics of formation of disulfide-bonded PDGF-AB dimers from unfolded and reduced PDGF-A and -B monomers. *A*, time course data of the relative concentrations of PDGF-A and -B monomers ( $\square$ ) and disulfide-bonded dimers ( $\blacksquare$ ) after subjecting an equimolar mixture of unfolded and reduced PDGF-A and -B chains to SEC under renaturing conditions. Time zero indicates the start of the kinetic experiment in the eluate fraction immediately after elution of monomeric PDGF-A and -B from the SEC column. *B*, determination of the rate constants assuming either a first-order ( $\bullet$ ) or a second-order rate-determining step ( $\circ$ ) as described under "Experimental Procedures." The experimental conditions were as follows:  $0.1 \text{ mol l}^{-1}$  Tris-HCl (pH 7.8),  $0.5 \text{ mol l}^{-1}$  GdnHCl,  $10 \text{ mmol l}^{-1}$  GSH,  $0.25 \text{ mmol l}^{-1}$  GSSG,  $8.9 \text{ } \mu\text{mol l}^{-1}$  ( $110 \text{ } \mu\text{g ml}^{-1}$ ) PDGF-A and -B monomers;  $T = 25^\circ\text{C}$ .

By rearranging the kinetic Equations 1 and 2, the monomer turnover  $U$  can be simulated assuming either a first-order (Equation 3) or a second-order rate-determining reaction (Equation 4).

$$1 - \frac{[A]_t}{[A]_0} = U = 1 - e^{-k_1[A]_0 t} \quad (\text{Eq. 3})$$

$$1 - \frac{[A]_t}{[A]_0} = U = 1 - \frac{1}{1 + [A]_0 k_2 t} \quad (\text{Eq. 4})$$

In case of a unimolecular rate-limiting reaction, the monomer turnover with time should be independent of the initial monomer concentration (Equation 3), while a second-order rate-limiting reaction should be reflected by an increased monomer turnover with increasing initial monomer concentration (Equation 4). Best-fit simulations of the data from kinetic experiments for the determination of the rate constants and modeling of the monomer turnover were carried out using standard software.

The temperature dependence of the rate of dimerization was described by an Arrhenius relationship, i.e. a plot of  $\ln k$  versus  $1/T$ ,

$$k = A \exp\left(\frac{\Delta S^\ddagger}{R}\right) \exp\left\{-\left(\frac{\Delta H^\ddagger}{R} - \frac{1}{T}\right)\right\} \quad (\text{Eq. 5})$$

where  $k$  is the experimentally determined rate constant,  $A$  is a constant in the activated complex theory,  $\Delta S^\ddagger$  and  $\Delta H^\ddagger$  the entropy and enthalpy

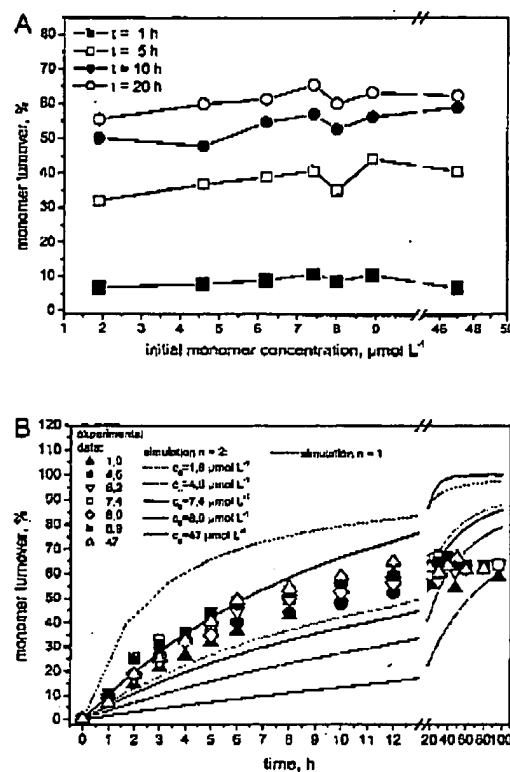


FIG. 3. Analysis of the monomer turnover for the determination of the reaction order of the rate-limiting step during the formation of disulfide-bonded PDGF-AB. *A*, determination of the monomer turnover at different time points with varying initial monomer concentrations: 1 h ( $\blacksquare$ ), 5 h ( $\square$ ), 10 h ( $\bullet$ ), and 20 h ( $\circ$ ) after eluting monomeric PDGF-A and -B from the SEC column. *B*, time course data of the monomer turnover of PDGF-A and -B starting with initial monomer concentrations of  $1.9 \text{ } \mu\text{mol l}^{-1}$  ( $\Delta$ ),  $4.6 \text{ } \mu\text{mol l}^{-1}$  ( $\bullet$ ),  $6.2 \text{ } \mu\text{mol l}^{-1}$  ( $\nabla$ ),  $7.4 \text{ } \mu\text{mol l}^{-1}$  ( $\square$ ),  $8.0 \text{ } \mu\text{mol l}^{-1}$  ( $\circ$ ),  $8.9 \text{ } \mu\text{mol l}^{-1}$  ( $\blacksquare$ ), and  $47 \text{ } \mu\text{mol l}^{-1}$  ( $\Delta$ ) are shown. In addition, best fit simulations are depicted assuming a first-order with  $k_1 = 1.5 \cdot 10^{-5} \text{ s}^{-1}$  (thick line) or a second-order rate-limiting step with  $k_2 = 2.5 \text{ mol}^{-1} \text{ s}^{-1}$  (for the renaturation of PDGF-AB:  $1.9 \text{ } \mu\text{mol l}^{-1}$  ( $23.5 \text{ } \mu\text{g ml}^{-1}$ ),  $\dots$ ;  $4.6 \text{ } \mu\text{mol l}^{-1}$  ( $56.9 \text{ } \mu\text{g ml}^{-1}$ ),  $---$ ;  $7.4 \text{ } \mu\text{mol l}^{-1}$  ( $91.5 \text{ } \mu\text{g ml}^{-1}$ ), thin line;  $8.9 \text{ } \mu\text{mol l}^{-1}$  ( $110 \text{ } \mu\text{g ml}^{-1}$ ),  $---$ ; and  $47 \text{ } \mu\text{mol l}^{-1}$  ( $581 \text{ } \mu\text{g ml}^{-1}$ ),  $---$ ). Experimental conditions were the same as described in the legend to Fig. 2 except for the initial concentrations of PDGF-A and -B monomers.

of activation of the reaction, respectively,  $T$  the temperature, and  $R$  the universal gas constant. If there is linearity for the temperature dependence of the rate constant, the enthalpy and entropy of activation can be determined from the slope and the y intercept of Equation 5, respectively.

## RESULTS

**Kinetics of Formation of Disulfide-bonded PDGF-AB Dimers from Unfolded and Reduced PDGF-A and -B Monomers**—The kinetics of the formation of disulfide-bonded dimers of PDGF were investigated under redox reshuffling conditions starting from an equimolar mixture of completely unfolded and reduced A- and B-chains (Fig. 2A). The kinetic data are well described either by assuming a first- or a second-order rate-determining reaction and the putative rate constants extracted from the slopes of the linearized kinetic equations (cf. experimental procedures) were determined to be  $k_1 = 1.5 \cdot 10^{-5} \text{ s}^{-1}$  or  $k_2 = 2.5 \text{ mol}^{-1} \text{ s}^{-1}$ , respectively (Fig. 2B).

To discriminate between a first- and a second-order rate-limiting reaction controlling the formation of disulfide-bonded

## Preferential Heterodimer Formation of Platelet-derived Growth Factor

18333

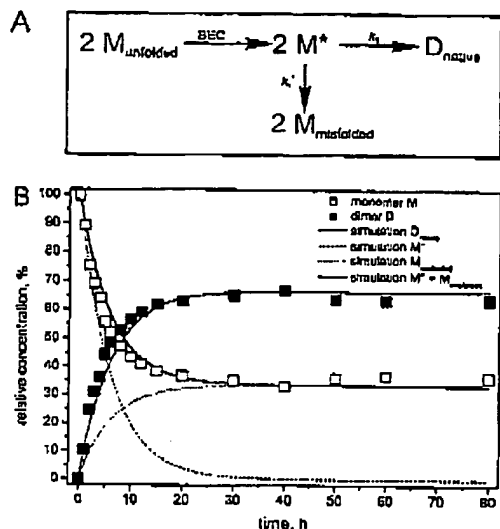


**FIG. 4. Simplified model for the formation of disulfide-bonded PDGF-AB dimers from unfolded and reduced PDGF-A and -B monomers.** A, simplified model for the formation of disulfide-bonded PDGF-AB dimers additionally including the formation of non-native off-pathway folding products  $M_{\text{misfolded}}$  incompetent for the formation of native disulfide-bonded PDGF-AB dimers. B, modeling of the kinetics assuming a first-order rate-limiting step with  $k_1 = 1.5 \cdot 10^{-5} \text{ s}^{-1}$  for the formation of the disulfide-bonded PDGF-AB dimer. Formation of  $M_{\text{misfolded}}$  is described assuming a first-order rate-limiting step with  $k_1' = 7.5 \cdot 10^{-6} \text{ s}^{-1}$ . In addition, the experimental time course data of the relative concentrations of PDGF-A and -B monomers ( $\square$ ) and disulfide-bonded dimers ( $\blacksquare$ ) are shown. Experimental conditions were the same as described in the legend to Fig. 2.

PDGF dimers, renaturation experiments were carried out with varying initial monomer concentrations (Fig. 3). The kinetic analysis revealed an independence of the monomer turnover at given time points on the initial monomer concentration (Fig. 3A), thus clearly excluding a second-order rate-limiting step in the renaturation of PDGF-AB. In addition, kinetic modeling revealed that the formation of the disulfide-bonded dimer is best described by a first-order rate-determining reaction (Fig. 3B). Deviation of the predicted monomer turnover from the experimental data originates from the formation of soluble off-pathway products, which are not able to form native PDGF-AB. To account for the incomplete monomer turnover, the kinetic model was further refined by including an additional step leading to the irreversible formation of misfolded off-pathway products (Fig. 4A). The experimental data are now well described by the productive first-order reaction with the rate constant of  $k_1 = 1.5 \cdot 10^{-5} \text{ s}^{-1}$  yielding the native disulfide-bonded PDGF-AB dimer and an unproductive reaction with a rate constant of  $k_1' = 7.5 \cdot 10^{-6} \text{ s}^{-1}$  leading to non-native off-pathway products (Fig. 4B).

A variation of the GdnHCl concentration between 0.25 and  $1.5 \text{ mol l}^{-1}$  in the renaturation buffer revealed a strong decrease in the rate of the formation of the disulfide-linked dimer with increasing concentrations of the chaotropic agent (Fig. 5). The graphic representation of the rate constants in a "chevron plot" revealed a linear dependence on the GdnHCl concentration by anticipating a first-order rate-limiting step for the generation of the disulfide-linked PDGF-AB dimer (Fig. 5B). Final yields of disulfide-linked PDGF-AB dimers increased from 13 to 75% by decreasing the concentration of GdnHCl from  $1.5$  to  $0.25 \text{ mol l}^{-1}$ . At  $2 \text{ mol l}^{-1}$  GdnHCl, formation of disulfide-linked dimers was not detectable (data not shown).

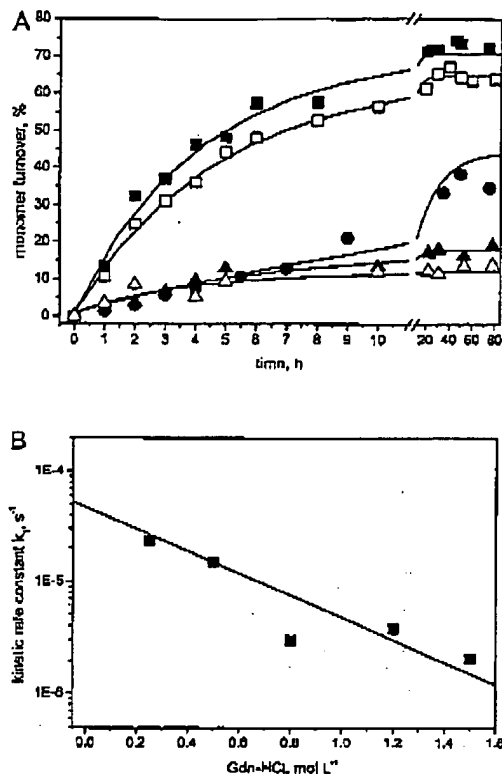


**FIG. 5. GdnHCl dependence of formation of disulfide-bonded PDGF-AB dimers from unfolded and reduced PDGF-A and -B monomers.** A, time-dependent monomer turnover of PDGF-A and -B at GdnHCl concentrations ranging from  $0.25$  to  $1.5 \text{ mol l}^{-1}$ :  $0.25 \text{ mol l}^{-1}$  GdnHCl ( $\blacksquare$ ),  $0.5 \text{ mol l}^{-1}$  GdnHCl ( $\square$ ),  $0.8 \text{ mol l}^{-1}$  GdnHCl ( $\bullet$ ),  $1.2 \text{ mol l}^{-1}$  GdnHCl ( $\triangle$ ), and  $1.5 \text{ mol l}^{-1}$  GdnHCl ( $\blacktriangle$ ). B, GdnHCl dependence of the kinetic rate constant  $k_1$  assuming a first-order rate-limiting reaction. Experimental conditions were the same as described in the legend to Fig. 2, except for the GdnHCl concentrations.

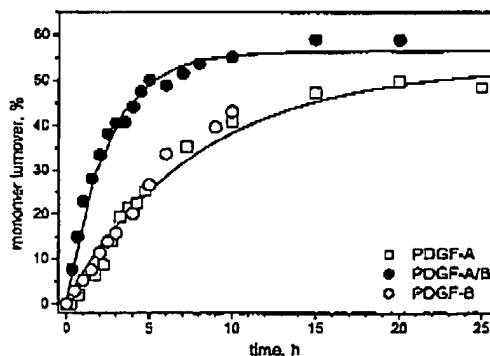


**FIG. 6. Kinetics of formation of disulfide-bonded PDGF dimers of the different PDGF isoforms from unfolded and reduced PDGF monomers.** The time-dependent monomer turnover of the three different PDGF isoforms PDGF-A, PDGF-A and -B, and PDGF-B are shown starting with initial monomer concentrations of:  $0.8 \mu\text{mol l}^{-1}$  PDGF-A ( $\square$ ),  $9.25 \mu\text{mol l}^{-1}$  PDGF-A and -B ( $\bullet$ ), and  $3.5 \mu\text{mol l}^{-1}$  PDGF-B ( $\circ$ ). Experimental conditions were the same as described in the legend to Fig. 2, except that the temperature was  $35^\circ\text{C}$ .

**Kinetics of Formation of Disulfide-bonded Dimers of the Different PDGF Isoforms—**A unimolecular rate-limiting reaction during the formation of the disulfide bonded PDGF dimer could

18334

## Preferential Heterodimer Formation of Platelet-derived Growth Factor

TABLE I  
Temperature dependence of the renaturation of the different PDGF isoforms  
Experimental conditions were the same as described in the legend to Fig. 7.

Temperature °C	First-order rate constant, $k_1$ $10^{-5} \text{ s}^{-1}$			Final yield %		
	PDGF-AA	PDGF-BB	PDGF-AB	PDGF-AA	PDGF-BB	PDGF-AB
4	0.03 ± 0.005	0.05 ± 0.005	0.06 ± 0.015	18	17	17
15	0.13 ± 0.005	0.17 ± 0.01	0.5 ± 0.1	25	45	55
25	0.5 ± 0.1	0.5 ± 0.05	1.5 ± 0.1	50	50	61
35	1.0 ± 0.1	1.0 ± 0.05	3.0 ± 0.2	50	51	59
45	1.0 ± 0.05	0.5 ± 0.05	2.0 ± 0.15	50	47	57

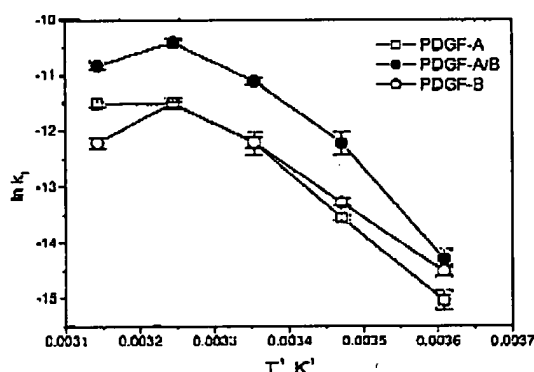


Fig. 7. Arrhenius plots of the rate constants of the formation of disulfide-bonded PDGF dimers of the different PDGF isoforms from unfolded and reduced PDGF monomers. The rate constants of dimerization of the three different PDGF isoforms PDGF-AA, PDGF-AB, and PDGF-BB were determined at temperatures ranging from 4 to 45 °C assuming a first-order rate-determining reaction. The initial monomer concentrations were: 0.8  $\mu\text{mol l}^{-1}$  PDGF-A ( $\square$ ), 9.25  $\mu\text{mol l}^{-1}$  PDGF-A and -B ( $\bullet$ ), and 3.5  $\mu\text{mol l}^{-1}$  PDGF-B ( $\circ$ ). Experimental conditions were the same as described in the legend to Fig. 2, except for the temperatures.

either indicate a rate-limiting folding reaction on the level of the monomeric chain or structural rearrangements on the level of the dimeric not yet disulfide-bonded growth factor. To discriminate between these two possibilities, a kinetic study of the formation of disulfide-bonded dimers was carried out using either the purified A- or B-chains or an equimolar mixture of both chains (Fig. 6). The formation of disulfide-bonded PDGF-AA or PDGF-BB homodimers displayed identical kinetics indicating that both monomeric forms as well as the dimerized homodimer have similar folding and assembly pathways. In contrast, disulfide-bonded heterodimers were formed three times more rapidly ( $k_1 = 1.5 \cdot 10^{-5} \text{ s}^{-1}$ , experimental conditions, cf. Fig. 6) compared with the formation of the two different disulfide-bonded homodimers from either pure A- or B-chains ( $k_1 = 0.5 \cdot 10^{-5} \text{ s}^{-1}$ , experimental conditions, cf. Fig. 6) when renaturation was started from an equimolar mixture of both chains.

At all temperatures ranging from 4 °C to 45 °C heterodimerization occurred more rapidly compared with the formation of homodimers (Fig. 7 and Table I), suggesting a general preference for the formation of the heterodimer. Also, the kinetics of homodimerization of the two different PDGF-AA or -BB isoforms did not show any significant difference in the temperature range studied, supporting the conclusion that homodimerization of either PDGF-AA or -BB follows most likely similar pathways.

During the renaturation of all the three different PDGF isoforms aggregation was not observed up to temperatures of 35 °C. However at 45 °C, partial aggregation of all PDGF isoforms occurred. A summary of the results from the renatur-

ation experiments carried out at the different temperatures is shown in Table I. An estimation of the activation enthalpies from the Arrhenius plots (Fig. 7; only data from 4 to 35 °C) of either homo- or heterodimerization did not reveal a significant difference for the different PDGF isoforms. Assuming a first-order rate-limiting renaturation step, activation enthalpies in the range of 70–80  $\text{kJ mol}^{-1}$  were estimated for the formation of PDGF-AA, -AB, or -BB.

## DISCUSSION

Subunit association can be a very fast process with rate constants in the order of  $10^7 \text{ mol}^{-1} \text{ l s}^{-1}$  (e.g. Ref. 25) that are encountered in diffusion-controlled reactions. However, when folding and association is connected with the formation of intra- and intermolecular disulfide bonds, e.g. during renaturation of antibody fragments, the regain of the biological activity can occur in the time scale of hours to days (26).

The formation of disulfide-bonded dimers of PDGF is also a very slow process occurring in the time scale of hours. Studies on the folding and association of brain-derived neurotrophic factor (18) and nerve growth factor (19), growth factors where the subunits are not connected by intermolecular disulfide bonds, also revealed slow renaturation kinetics, although, in general, little information exists on the folding and association pathways of dimeric proteins of the cystine knot growth factor family.

The rate-limiting step during the renaturation of a dimeric protein can either be a first-order step resulting from unimolecular conformational changes or a second-order step originating from the encounter and assembly of the subunits. The experimental results clearly show that the formation of the PDGF dimer is a process controlled by a first-order reaction, thus proving that the encounter of the monomeric chains to form the dimeric growth factor is not the rate-limiting step in the renaturation of PDGF. A first-order rate-determining reaction during the renaturation of a multimeric protein is not unusual. For example, the kinetic analysis of the renaturation of the homodimeric mitochondrial malate dehydrogenase revealed a second-order association reaction (27), whereas the renaturation kinetics of the cytoplasmic enzyme, also a homodimer, were governed by a first-order rate-limiting step (28).

A first-order rate-limiting reaction can result from folding events on the monomer level or from structural rearrangements of an already dimerized protein. The comparative analysis of homo- and heterodimerization revealed identical kinetics for the formation of the disulfide-bonded AA or BB homodimers, suggesting that their renaturation pathways do not differ significantly, e.g. that folding of the two different monomeric chains into association competent molecules, association of these monomers into homodimers, and, finally, formation of intermolecular disulfide bridges do not exhibit significantly different pathways when renaturation was started either from the unfolded and reduced pure A- or B-chains. In contrast, the AB heterodimers were formed three times more rapidly compared with the formation of the homodimers. As-

## Preferential Heterodimer Formation of Platelet-derived Growth Factor

18335

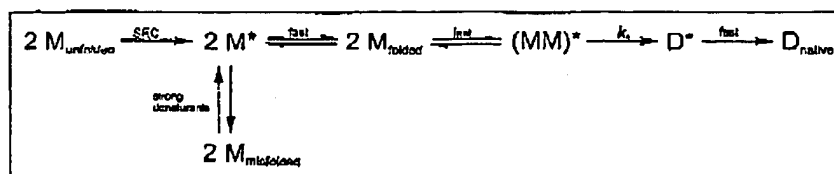


FIG. 8. Basic model for the formation of disulfide-bonded PDGF dimers from unfolded and reduced PDGF monomers. In this scheme  $M_{\text{unfolded}}$  represents the unfolded and reduced PDGF monomers, which are subjected to SEC under conditions allowing refolding and disulfide bond reshuffling.  $M^*$  signifies the PDGF monomer recovered directly after SEC in the eluate fraction. The reaction includes the transformation of  $M^*$  into association competent monomers  $M_{\text{folded}}$ , the subsequent encounter of  $M_{\text{folded}}$  with another  $M_{\text{folded}}$  into a non-covalently associated dimer  $(MM)^*$ , the first-order rate determining structural rearrangements yielding the not yet disulfide-bonded dimer  $D^*$ , which can be transformed through intermolecular disulfide-bonding into the native growth factor  $D_{\text{native}}$ . The model additionally includes the formation of non-native off-pathway folding products  $M_{\text{misfolded}}$  incompetent for the formation of native disulfide-bonded PDGF dimers.

suming a rate-determining first-order step on the level of monomer folding and observing identical homodimerization kinetics is not contradictory if both monomeric isoforms exhibit identical folding kinetics prior to the formation of the dimer. But a rate-determining first-order step on the level of monomer folding should also result in the same kinetics for homo- and heterodimerization if both monomeric isoforms exhibit identical folding kinetics. However, we observe that heterodimerization of PDGF-AB occurs three times more rapidly than homodimerization. These results clearly exclude the possibility that the rate-determining first-order step can be assigned to conformational folding steps on the level of the not yet dimerized monomer but point clearly to structural rearrangements on the level of the dimerized but not yet disulfide-bonded dimer as the pace maker of renaturation. In this case, the different monomers can fold on identical pathways as the experimental results strongly suggest; however, once dimerized but not yet disulfide-bonded, the formation of the cystine bonds between the different chains must be facilitated between the PDGF-A and -B monomer compared with disulfide-bonding between identical chains. The results also show that a statistically and diffusion controlled encounter of the different monomers must be reversible, i.e. that non-covalent monomer association and dissociation must occur prior to the formation of intermolecular disulfide bonds under the conditions studied. Once connected by intermolecular disulfide bonds, however, there are no indications for subunit exchange processes (data not shown). The results from the kinetic studies on the folding and assembly of PDGF are summarized in the model depicted in Fig. 8.

The kinetically preferred formation of the heterodimeric growth factor should also affect the isoform distribution. Statistically an isoform distribution of 1:2:1 is expected when refolding occurs from an equimolar mixture of A- and B-chains. However, three times faster heterodimerization compared with homodimerization should result in an isoform distribution of 1:6:1, which accounts for 12.5% PDGF-AA, 75% PDGF-AB, and 12.5% PDGF-BB. A similar isoform distribution was reached when Chinese hamster ovary cells were used for coexpression of the genes encoding the PDGF-A and -B chains (19% AA, 69% AB, and 12% BB; Ref. 29).

The strong dependence of the kinetic constant of the rate-limiting renaturation step on the concentration of the denaturant GdnHCl strongly suggests that general structural rearrangements on the level of the non-covalently associated but not yet disulfide-bonded dimer determine the speed of renaturation. Finally, similar activation enthalpies of hetero- and homodimerization indicate that preferential heterodimerization must be controlled by entropic factors resulting in a more

favorable positioning of the cysteines from different chains for the formation of the intermolecular disulfide bonds compared with disulfide bond formation between identical chains.

**Acknowledgment**—We are grateful to F. X. Schmid for useful comments concerning the interpretation of the Arrhenius plot data.

## REFERENCES

1. Rasmussen, R., Raines, E. W., and Bowen-Pope, D. F. (1986) *Cell* 46, 155–160
2. Heldin, C.-H. (1992) *EMBO J.* 11, 4251–4259
3. Meyer-Ingold, W., and Eichner, W. (1996) *Cell Biol. Int.* 19, 389–398
4. Meyer-Ingold, W. (1993) *Trends Biotechnol.* 11, 387–392
5. Isaacs, N. W. (1996) *Curr. Opin. Struct. Biol.* 5, 381–395
6. Gilbertson, D. G., Duff, M. E., West, J. W., Kelly, J. D., Sheppard, P. O., Hofstrand, P. D., Gao, Z., Shoemaker, K., Rukowatski, T. R., Moore, M., Feldhaus, A. L., Humes, J. M., Palmer, T. E., and Hart, C. E. (2001) *J. Biol. Chem.* 276, 27406–27414
7. LaRoche, W. J., Jeffers, M., McDonald, W. F., Chilkoturu, R. A., Giese, N. A., Lecker, N. A., Sullivan, C., Boldog, F. L., Yang, M., Vernet, C., Burgess, C. E., Fernandes, E., Dongler, L. L., Rittman, B., Shinkov, J., Shinkov, R. A., Rothberg, J. M., and Lieberstein, H. S. (2001) *Nat. Cell Biol.* 3, 617–621
8. Rothholz, C., Johnson, A., Heldin, C.-H., Westermarck, B., Lind, P., Urdan, M. S., Eddy, R., Shows, T. B., Philpott, K., Mellor, A. L., Knott, T. J., and Scott, J. (1988) *Nature* 330, 606–609
9. Hannink, M., and Donoghue, D. J. (1989) *Biochim. Biophys. Acta* 989, 1–10
10. Heldin, C. H., and Westermarck, B. (1989) *Trends Genet.* 5, 108–111
11. Hammacher, A., Hellman, U., Johnson, A., Ostman, A., Gunnarsson, K., Westermarck, B., Westerman, A., and Heldin, C.-H. (1988) *J. Biol. Chem.* 263, 16493–16498
12. Hoppe, J., Weich, H. A., Eichner, W., and Tüjse, D. (1990) *Eur. J. Biochem.* 187, 207–214
13. Schneppe, B., Eichner, W., and McCarthy, J. E. G. (1994) *Gene (Amst.)* 143, 201–209
14. Müller, C., and Rinas, U. (1999) *J. Chromatogr. A* 866, 203–213
15. Oefner, C., D'Arcy, A., Winkler, F. A., Eggmann, B., and Hoesang, M. (1992) *EMBO J.* 11, 3921–3926
16. Juenicke, R., and Rudolph, R. (1986) *Methods Enzymol.* 131, 218–250
17. Juenicke, R. (1991) *Biochemistry* 30, 3147–3161
18. Philpott, J. S., Rosenfeld, R., Arakawa, T., Wen, J., and Narhi, L. O. (1999) *Biochemistry* 38, 10812–10818
19. Rattenhall, A., Ruoppolo, M., Flagiello, A., Monti, M., Vinci, F., Marino, C., Lillo, H., Schwarz, E., and Rudolph, R. (2001) *J. Mol. Biol.* 305, 523–533
20. Müller, Y. A., Hoising, C., Missolwitz, R., Welfe, K., and Welfe, H. (2002) *J. Biol. Chem.* 277, 43410–43418
21. Kenney, W. C., Haniu, M., Herman, A. C., Arakawa, T., Costigan, V. J., Lary, J., Yphantis, D. A., and Thomson, A. R. (1994) *J. Biol. Chem.* 269, 12351–12359
22. Prestrelak, S. J., Arakawa, T., Duker, K., Kenney, W. C., and Narhi, L. O. (1994) *Int. J. Pept. Protein Res.* 44, 357–363
23. Raines, E. W., and Ruse, R. (1986) *Methods Enzymol.* 108, 743–778
24. Saege, A., Schneppe, B., McCarthy, J. E. G., Deckwer, W.-D., and Rinas, U. (1996) *Enzyme Microb. Technol.* 17, 947–953
25. Mill, M. E., and Sauer, R. T. (1994) *Biochemistry* 33, 1125–1133
26. Buchner, J., and Rudolph, R. (1991) *Bio/Technology* 9, 157–162
27. Juenicke, R., Rudolph, R., and Heider, I. (1979) *Biochemistry* 18, 1217–1228
28. Rudolph, R., Fuchs, L., and Juenicke, R. (1986) *Biochemistry* 25, 1662–1669
29. Ostman, A., Rall, L., Hammacher, A., Westermarck, M. A., Cui, D., Valenzuela, P., Rothholz, C., Westermarck, B., and Heldin, C.-H. (1988) *J. Biol. Chem.* 263, 16202–16208
30. Scheufler, C., Sebald, W., and Hülsmeyer, M. (1999) *J. Mol. Biol.* 287, 103–115
31. Hinc, A. P., Archer, S. J., Qian, S. W., Roberts, A. R., Sporn, M. B., Weatherbee, J. A., Tsang, M. L.-S., Jacobs, R., Zhang, B.-L., Wenker, J., and Torchia, D. A. (1996) *Biochemistry* 35, 8517–8524